The pCO_2 variability in the midlatitude North Atlantic Ocean during a full annual cycle

Heike Lüger, Douglas W. R. Wallace, and Arne Körtzinger

Marine Biogeochemie, Leibniz-Institut für Meereswissenschaften, Institute for Marine Research (IFM-GEOMAR), Kiel, Germany

Yukihiro Nojiri

National Institute for Environmental Studies (NIES), Tsukuba, Ibaraki, Japan

[1]   The results of 1 year of automated pCO_2 measurements in 2002/2003 onboard the car carrier M/V *Falstaff* are presented and analyzed with regard to the driving forces that change the seawater pCO_2 in the midlatitude North Atlantic Ocean. The pCO_2 in surface seawater is controlled by thermodynamics, biology, air-sea gas exchange, and physical mixing. Here we estimate the effects on the annual cycle of pCO_2 and relate this property to parameters like SST, nitrate, and chlorophyll. On the basis of the amplitude in seawater pCO_2 for all $4° \times 5°$ grid boxes, this region can be separated into an eastern and western basin. The annual pCO_2 cycle in the eastern basin ($10°W–35°W$) is less variable, which can be related to the two counteracting effects of temperature and biology; air-sea gas exchange plays a minor role when using climatological MLD. In the western basin ($36°W–70°W$) the pCO_2 amplitude is more variable and strongly follows the thermodynamic forcing, since the biological forcing (as derived from nitrate concentrations) is decreased. Biology and air-sea exchange strongly depend on the MLD and therefore also include physical mixing effects. The pCO_2 data of the analyzed region between $34°N$ and $52°N$ compare well to the *Takahashi et al.* [2002] climatology except for regions north of $45°N$ during the wintertime where the bias is significant.   *INDEX TERMS:* 4227 Oceanography: General: Diurnal, seasonal, and annual cycles; 4805 Oceanography: Biological and Chemical: Biogeochemical cycles (1615); 4806 Oceanography: Biological and Chemical: Carbon cycling; 4835 Oceanography: Biological and Chemical: Inorganic marine chemistry *KEYWORDS:* carbon cycle, North Atlantic Ocean, seawater pCO_2, VOS

1.   Introduction

1.1.   Scientific Background

[2]   Since the onset of major agricultural changes and the industrial revolution the CO_2 content in the atmosphere has increased by 30%. CO_2 is the most important anthropogenically affected greenhouse gas and leads to increased radiative forcing [*Houghton et al.*, 1996], thus potentially changing the global climate. Possible impacts of this global climate change cannot be fully appreciated as of now; one of the reasons is the limited understanding of the global carbon cycle and the future role of the ocean. A central question is how much anthropogenic CO_2 is taken up by ocean and land now and in the future. Current estimates of the uncertainty of the ocean uptake term are 0.8 PgC yr^{-1}, which is a fourfold uncertainty compared to atmospheric measurements [see also *Wallace*, 2001]. Calculation of the

oceanic CO_2 flux from the atmosphere-ocean CO_2 partial pressure difference (ΔpCO_2) is not straightforward and involves several sources of error. Furthermore, the seasonal variability of the seawater pCO_2 is difficult to assess, because direct measurements are sparse. It has been the focus of many research projects to explain the variability of oceanic pCO_2 by a number of parameters: sea surface temperature [e.g., *Lefèvre and Taylor*, 2002; *Lefèvre et al.*, 1994; *Boutin et al.*, 1999; *Stephens et al.*, 1995], SST anomaly [*Etcheto et al.*, 1999], sea surface salinity and temperature [*Weiss et al.*, 1982], physical transports [e.g., *Dandonneau*, 1995; *Winn et al.*, 1994], air-sea exchange [*Lefèvre et al.*, 1994], and phytoplankton blooms [*Watson et al.*, 1991; *Takahashi et al.*, 1993]. Predicting the pCO_2 from changes in SST and SSS is generally most successful in oligotrophic areas such as the subtropical gyres of the North Pacific and Atlantic, especially if the correlation is resolved seasonally [*Bates et al.*, 1996]. In areas with higher biological productivity such as temperate and subpolar seas, however, the pCO_2 is stronger affected by biological
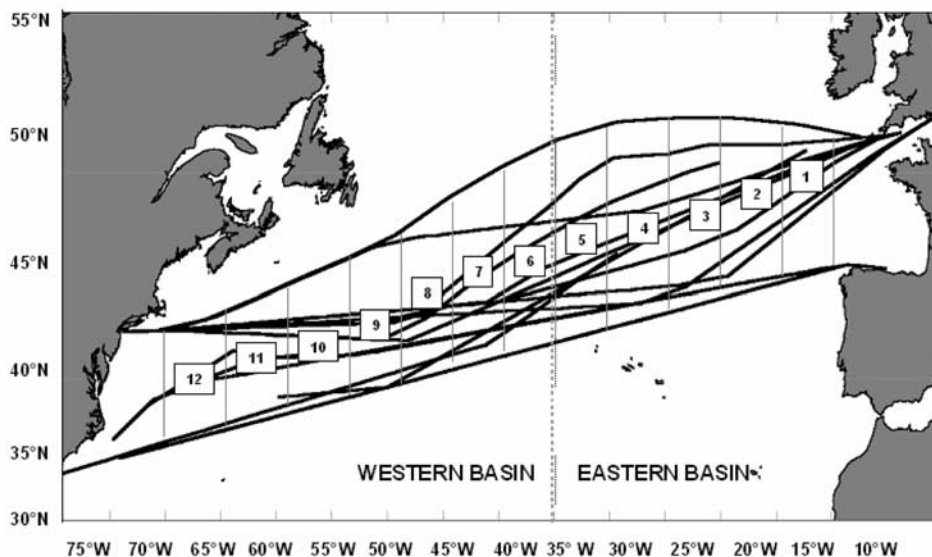
Figure 1. Cruises of M/V *Falstaff* between February 2002 and January 2003. The shaded lines delineate the borders of the 12 grid bands that were used in the data analysis for estimating seasonal cycles of pCO_2 and related parameters from observations. Data from marginal seas were excluded (see text). The dotted line indicates the boundary between the eastern ($10°W-35°W$) and western ($36°W-70°W$) basin as determined by the distinctively different pCO_2 seasonality in both domains.

drawdown [*Watson et al.*, 1991] and correlations with SST/SSS become much weaker. Strong seasonality in the vertical mixing also plays an important role in these areas, as has been shown for the North Pacific [*Sasai et al.*, 2000].

[3] All approaches that are concerned with the seasonal variability of the seawater pCO_2 show the need of thorough data sampling. Much effort has been made to establish an ocean-wide network that can monitor changes in pCO_2 and related parameters. Especially in the Pacific, results from regular measurements onboard commercial vessels are promising [*Nojiri et al.*, 1999; *Zeng et al.*, 2002]. In the Atlantic Ocean a comparable network was initialized by them European project CAVASSOO (Carbon Variability Studies by Ships of Opportunity) in 2001. This project encompassed three commercial and one research vessel on which seawater and atmospheric pCO_2, SST, and SSS were continuously monitored. All lines were operating with onboard pCO_2 measurement units that collected data continuously. Furthermore, on many cruises, discrete samples for parameters such as nutrients, dissolved inorganic carbon, total alkalinity, chlorophyll *a*, etc., have been collected. This includes data for winter months for which historical data in the northern North Atlantic are extremely sparse.

[4] Here we present results covering a full annual cycle between February 2002 and January 2003 obtained from the Swedish car carrier M/V *Falstaff*. The data are used to analyze the seasonal development of the seawater pCO_2 within the eastern and western basin of the North Atlantic. Correlations between the seawater pCO_2 and SST, nutrients and other parameters are examined and used to identify and explain primary factors controlling the seasonal variability. Also, basin-wide estimates of the temperature, biology, and air-sea gas exchange effects on the seawater pCO_2 are made

in an attempt to explain their variability throughout the year. We compare and discuss our observations with reference to the climatology of *Takahashi et al.* [2002], which is based on historical data.

1.2. Hydrography of the Midlatitude North Atlantic

[5] The cruises covered a geographical area of the North Atlantic which ranges from $34°N$ to $54°N$ and $10°W$ to $70°W$ (Figure 1). *Wright and Worthington* [1970] identified four main basins in the North Atlantic (north of $20°N$): Labrador, European, North American, and North African basins. The western basins (Labrador and North American basin) are separated from the eastern basins by the Mid-Atlantic Ridge. Two main upper ocean water masses ($0-500$ m) are the Eastern and the Western North Atlantic Central Water [*Hinrichsen and Tomczak*, 1993]. These water masses exhibit a different physical but also biological behavior.

[6] The western part is dominated by the Gulf Stream system (subtropical gyre). Here, at low to midlatitudes, wind stirring is important for the nutrient distribution in the water column since it destratifies the water column and brings up nutrient-rich waters to the surface. Increase in nutrient concentrations plus adequate light conditions promote phytoplankton growth. Furthermore eddies play an important role in redistributing chemical and physical parameters especially at the northwest boundary. During summer months, however, a strong stratification of the water column prevents further vertical supply of nutrients. In the northeast (subpolar gyre), winter convection plays a crucial role [*Emery and Meincke*, 1986]. Deep convection at high latitudes ($>40°N$) prevents phytoplankton growth due to severely decreased light levels. During the seasonal warming and concurrent stratification of the

Table 1. *Falstaff* Cruises Between February 2002 and January 2003[a]

Cruise Number	Time	Maximum Latitude	Minimum Latitude	Minimum Longitude	Maximum Longitude	Samples (Discrete)
FAL01	Feb. 2002	50°N	41°N	2°W	67°W	nuts/Chl
FAL02	March 2002	41°N	38°N	40°W	67°W	
FAL03	April 2002	49°N	41°N	20°W	71°W	nuts/Chl
FAL04	May 2002	50°N	37°N	12°W	60°W	
FAL05	May 2002	50°N	41°N	5°W	71°W	nuts/Chl
FAL06	June 2002	44°N	35°N	10°W	73°W	
FAL07	July 2002	50°N	41°N	5°W	70°W	nuts/Chl
FAL08	July 2002	43°N	34°N	13°W	73°W	
FAL09	Aug. 2002	50°N	41°N	5°W	73°W	nuts/Chl
FAL11	Sept. 2002	50°N	41°N	4°W	73°W	nuts/Chl
FAL12	Oct. 2002	44°N	33°N	5°W	75°W	
FAL13	Nov. 2002	51°N	40°N	1°W	74°W	nuts/Chl
FAL14	Nov. 2002	44°N	33°N	29°W	80°W	
FAL15	Dec. 2002	50°N	41°N	5°W	70°W	nuts/Chl
FAL16	Jan. 2002	44°N	35°N	10°W	75°W	nuts/Chl

[a]On all cruises seawater and atmospheric pCO$_2$, SST, and SSS were measured continuously (nuts: discrete nutrient and CT/TA samples; Chl: discrete chlorophyll a samples).

surface ocean, strong phytoplankton blooms are promoted by the wintertime buildup of surface nutrients and optimal light conditions [*Yoder and Kennelly*, 2003].

2. Methods

2.1. Data Collection and Analytical Methods

[7] In January 2002, the M/V *Falstaff* was outfitted for automated shipboard measurements of pCO$_2$ and related parameters. From February 2002 to January 2003 the M/V *Falstaff* sailed across the North Atlantic 15 times. One roundtrip usually took 6 weeks, including several port calls in Europe and U.S. east coast, with a mean cruising speed of 18 knots at sea. Continuous measurements of seawater pCO$_2$, temperature, and salinity were performed on all cruises. The navigation data (UTC-time, geographical position) were retrieved from a GPS receiver installed on the upper deck of the ship. Here we also installed the air inlet through which we pumped air down to the measurement unit located in the ship's engine room for the determination of atmospheric CO$_2$. In addition to these continuous measurements, we also manually collected discrete samples for various parameters including nutrients and chlorophyll a on every second cruise (Table 1).

[8] The seawater inlet was installed at the ship's starboard sea chest located in the engine room of the ship (~6 m below waterline). Temperature and salinity were measured by a thermosalinograph (model 21 Seacat, Seabird Electronics Inc., Seattle, Washington) with the remote temperature sensor installed at the seawater inlet. The seawater is warmed on average by about 0.04°C on the way from the inlet to the equilibrator, and the seawater pCO$_2$ data have been corrected for this. The SST and SSS data were recorded every 6 s, merged with the navigation data and stored as 1-min averages.

[9] After passing through the thermosalinograph the seawater flows into the pCO$_2$ measurement unit. This system was designed jointly by one of us (Y. Nojiri) and Kimoto Inc. (both Japan). The seawater flows at a rate of ~20 L min^{-1} into the equilibrator, where it is brought into contact with a countercurrent airflow. The equilibrator

(Japanese Patent P2001-83053A) is a tandem type with two stages: The seawater enters from the top into a shower-type upper stage which is mounted on top of the bubble-type lower stage. The countercurrent airflow enters from below. Any equilibration bias introduced due to the hydrostatic pressure exerted on the gas bubbles during passage through the bubble stage (equilibration efficiency 99.5%) is largely removed in the shower stage (equilibration efficiency 90%). The overall equilibration efficiency of 99.95% has been determined in various laboratory tests and was confirmed during an indoor pool experiment in Tsukuba, Japan, in March 1999, using varying pool conditions as well as different CO$_2$ concentrations of the countercurrent air supply for the equilibrators. After passage through the equilibration unit, the seawater drains into a reservoir. Finally, the seawater is actively pumped outside of the ship from the reservoir.

[10] The system is operated at atmospheric pressure, thus preventing any pressure gradient that might bias the pCO$_2$ determination. After equilibration with the seawater pCO$_2$, only a part of the countercurrent airflow is subsequently pumped into the CO$_2$ analysis unit. The other part of the airflow is vented through the equilibrator vent. A small air reservoir in the vent line prevents invasion of engine room air due to water level changes in the equilibrator during heavy sea. Otherwise the resulting "breathing" of the equilibrator might cause significant biases due to elevated CO$_2$ levels in the engine room air. Prior to analysis, the air is treated and dried in several steps which include aerosol filters, a Peltier cooling element, Nafion® tubing, and a magnesium perchlorate trap. Finally, the mole fraction of CO$_2$ (xCO$_2$) is measured once per minute by a nondispersive infrared (NDIR) detector (LiCOR®, model 6252, Lincoln, Nebraska).

[11] Since the equilibration takes place at ambient atmospheric pressure as measured by the barometer within the analysis unit, the pressure reading is used to correct xCO$_2$ into pCO$_2$. This pressure reading as measured in the engine room was compared to the shipboard barometer which is installed on the bridge. The accuracy of the shipboard barometer is about ±3 mbar. After height

correction, the barometric reading from the pCO_2 system in the engine room (6 m below sea level) and from the ship's bridge agree within the 3-mbar error. Any possible engine room overpressure of up to 3 mbar would result in a pCO_2 error on the order of ≤ 1 μatm.

[12] The analysis cycle involves a calibration cycle every 6 hours during which a suite of three standard gases (nominal concentrations: 250, 350, and 450 ppm CO_2 in natural air) is measured. These working standard gases were calibrated against NOAA primary standards (accuracy: 0.07 ppm) with similar concentration ranges using a LiCOR® NDIR analyzer (model 6262). After each calibration run, atmospheric air is measured for 20 min, and this is repeated every 2 hours. The seawater pCO_2 is measured during the remaining time (approximately 880 min/day). The raw voltage readings of the NDIR are corrected for temperature and pressure effects [Dickson and Goyet, 1994] using a least squares procedure for the quadratic regression function. The partial pressure of CO_2 (pCO_2) is calculated as follows:

$$pCO_2 = (P - pH_2O) \times xCO_2, \qquad (1)$$

where P is barometric pressure, pH_2O is the water vapor pressure, and xCO_2 is the measured dry air CO_2 mole fraction.

[13] On 10 cruises throughout the year, nutrient, total dissolved carbon (DIC), total alkalinity (TA), and chlorophyll samples were taken every 3 to 6 hours (Table 1). The nutrient samples were kept frozen and analyzed in the shore-based laboratory at the IfM-GEOMAR, Kiel, following the method of Hansen and Koroleff [1999]. The accuracy of the nitrate determination is $\pm 3\%$ in the range 0–10 μmol L^{-1}. DIC and TA samples were preserved with 0.02% (by volume) saturated $HgCl_2$ solution onboard the vessel following DOE instructions. DIC was analyzed with the coulometric technique of Johnson et al. [1999] using a SOMMA system. TA samples were analyzed by the potentiometric titration in an open cell as described by Mintrop et al. [2000]. Both DIC and TA samples were calibrated against certified reference material provided by A. Dickson (Scripps Institution of Oceanography, La Jolla, USA). The precision (accuracy) was ± 2 (± 1) μmol kg^{-1} for the DIC and ± 2 (± 2) μmol kg^{-1} for the TA analysis.

[14] Samples for chlorophyll a (1–2 L) were filtered onboard using glass fiber filters (Whatman GF/F), which were also stored frozen prior to analysis in Kiel. Chlorophyll a was determined at the IfM-GEOMAR using the spectrophotometric method by Jeffrey and Humphrey [1975] with an estimated accuracy of $\pm 5\%$.

2.2. Data Analysis
2.2.1. The pCO_2 Calculation and Gridding

[15] One year of observations was used to create monthly maps of seawater and atmospheric pCO_2 and SST. The data from each cruise were first averaged into 12 meridional bands of 5° width in longitude and varying zonal extent (Figure 1). These bands have a maximal latitudinal range of 10°. Ocean regions east of 10°W and

west of 70°W were excluded from the calculation in order to remove coastal influences.

[16] After Zeng et al. [2002], the seasonality of both seawater and atmospheric pCO_2 and SST were analyzed for each 5° longitudinal band with a sigmoidal function which can be expressed by a harmonic equation. The latter was computed for each 5° longitude band:

$$x(t) = c_0 + c_1 \sin(2\pi t) + c_2 \cos(2\pi t) + c_3 \sin(4\pi t) + c_4 \cos(4\pi t), \qquad (2)$$

where x is the seasonally varying quantity (e.g., pCO_2), t is time (in months) and $c_1 - c_4$ are four seasonal terms. It is required for good seasonal coverage that the maximum data gap should not exceed 3 months.

[17] To estimate the statistical error of this fitting procedure, we compared the seasonal function with the observed data (Figure 2a). The regression of the geometric mean of observed and fitted data yields the following equation:

$$\left(pCO_{2,\text{fitted}}\right) = 0.83(\pm 0.03)pCO_{2,\text{observed}} + 58.2(\pm 14) \ \ R^2 = 0.83. \qquad (3)$$

[18] We retrieved a deviation of 0.82 from the 45° line which shows that the agreement is good between observed and fitted data. There is a negligible offset in the residuals (mean = 0.00004), and the standard deviation of the difference is ± 9.47 (Figure 2b). The distribution of the residuals (fitted − observed data) shows neither a spatial nor a temporal trend (not shown).

2.2.2. Temperature and Nontemperature Effects on the Seawater pCO_2

[19] An objective of this work is to determine and quantify temperature and nontemperature related effects on surface seawater pCO_2 in the midlatitude Atlantic Ocean. We calculate the seasonal amplitudes of the pCO_2 which can help to distinguish between forced primarily by temperature variability and regions forced by other factors, for example, biological productivity and mixed layer depth variability [Takahashi et al., 2002]. As a convention, the seasonal pCO_2 amplitude is assigned a negative value if the annual maximum pCO_2 is found during winter (factor: −1). A positive sign is assigned to the pCO_2 amplitude if the annual maximum pCO_2 value is found during summer (factor: +1). Note that winter and summer are defined as the 6-month periods November–April and May–October, respectively.

[20] The results of this computation (Figure 3) show a seasonal pCO_2 amplitude that ranges between −21 and −30 μatm in the eastern North Atlantic, whereas positive values of +28 to +74 μatm are found in the western North Atlantic. On the basis of this marked regional difference, we separated the North Atlantic into two separate regimes: an eastern and a western basin comprising the region from 10°W to 35°W and 36°W to 70°W, respectively. Note that the same separation, eastern versus western seasonality, is obvious in the climatological pCO_2 data of Takahashi et al. [2002] (Figure 3). This supports our choice of dividing the
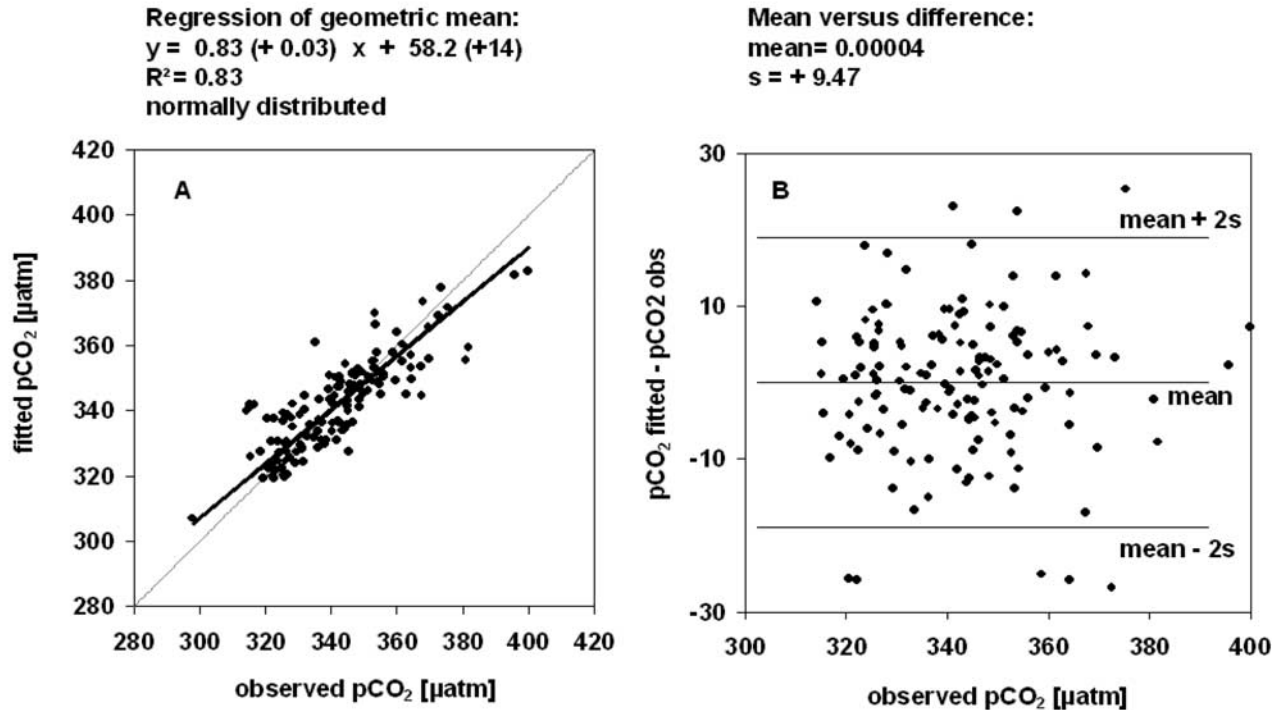
Figure 2. Comparison of observed and fitted seawater pCO_2. The observed data were averaged to 5° longitudinal grid bands of varying zonal extent. The fitted data were computed using equation (2). (a) Geometric mean of observed and fitted data yields: $y = 0.83x + 58.2$ ($R^2 = 0.83$). Both observed and fitted data are normally distributed. (b) Residuals plotted against the mean of observed pCO_2. The black lines indicate the mean and the 2σ margins.

region into two provinces showing a distinct difference in the seasonality of the seawater pCO_2.

[21] We parameterize temperature and nontemperature related effects on the seawater pCO_2 according to the following equations [*Takahashi et al.*, 2002]:

Temperature-dependent pCO_2

$$pCO_2(T_{obs}) = pCO_{2,mean} \times e^{0.0423(T_{obs}-T_{mean})} \qquad (4)$$

Temperature-independent pCO_2

$$pCO_2(T_{mean}) = pCO_{2,obs} \times e^{0.0423(T_{mean}-T_{obs})}, \qquad (5)$$

where $pCO_{2,mean}$ denotes the observed annual mean seawater pCO_2 per grid band, $pCO_{2,obs}$ represents the observed monthly mean seawater pCO_2 per grid band, and T_{mean} and T_{obs} are the observed annual and monthly mean SST values per grid band, respectively. In effect, equation (4) modulates the annual mean pCO_2 values according to the seasonal SST cycle, thus accounting for the pure thermodynamic effect of temperature on the solubility of dissolved CO_2 and the speciation of CO_2 system (4.23% change per 1°C; [*Takahashi et al.*, 1993]). The result represents the seasonal pCO_2 signal if this was only driven by temperature. In contrast, equation (5) corrects the observed seawater pCO_2 for the temperature effect and thus reveals any remaining seasonal pCO_2 variability that is

not accounted for by the seasonal SST cycle. The result of this deconvolution thus represents changes in seawater pCO_2 values that are forced by factors such as biological production, air-sea gas exchange, or lateral/vertical mixing.

2.2.3. Temperature, Biology, and Air-Sea Exchange Effects on the Seawater pCO_2

[22] In this section we estimate the effects of temperature change, "biological" carbon drawdown, and air-sea exchange of CO_2 on the air-sea ΔpCO_2 ($=pCO_{2,seawater} - pCO_{2,atmosphere}$) in the eastern and western basins of the North Atlantic following the approach of *Lefèvre et al.* [1994]. The thermally driven monthly pCO_2 change, $\Delta pCO_{2,temp}$, has been calculated by

$$\Delta pCO_{2,temp} = pCO_{2,pm} \times e^{0.0423(T_m - T_{pm})} - pCO_{2,pm}. \qquad (6)$$

The "biologically" driven monthly change of the seawater pCO_2, $\Delta pCO_{2,bio}$, is calculated from the monthly nitrate change which is converted into a DIC change by using a Redfield ratio of 7.2 for the North East Atlantic [*Körtzinger et al.*, 2001]. Please note that we assume the resulting $\Delta pCO_{2,bio}$ to represent the monthly change in pCO_2 driven by "biological" carbon drawdown as mirrored in changes in nitrate concentrations. We are aware, however, that monthly nitrate changes not only depend on local uptake, but also on lateral advection and vertical mixing. Therefore the "biologically" driven pCO_2 change may be biased to the
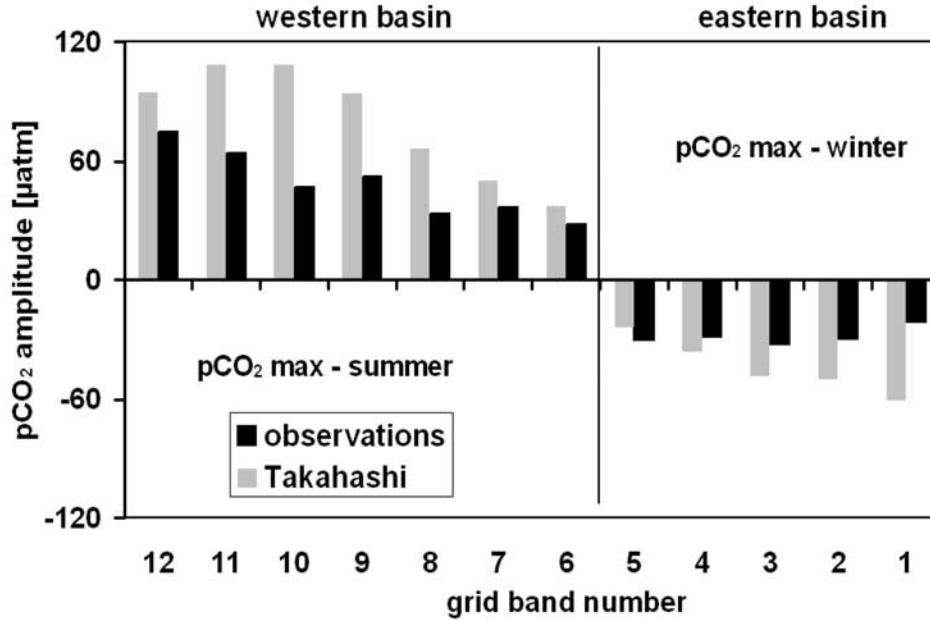
Figure 3. Seasonal amplitude of the seawater pCO$_2$ of all 12 latitudinal grid bands based on observations (black) and the climatological data set (shading) by *Takahashi et al.* [2002]. The data were computed according to *Takahashi et al.* [2002]: A positive sign is assigned when the maximum seawater pCO$_2$ occurs in the warm season (here: western basin). A negative sign of the amplitude refers to a grid band where the maximum seawater pCO$_2$ occurs during the cold season (here: eastern basin). A clear delineation between a western (summer pCO$_2$ maximum) and eastern (winter pCO$_2$ maximum) domain is found for both data sets.

extent that nitrate changes due to lateral advection and vertical mixing are not accompanied by the respective Redfield DIC-equivalent. Keeping this in mind, we still think that this rather simplistic approach is a helpful exercise to contrast the thermodynamic effects with "biological" effects on the observed pCO$_2$ variability. Therefore we use quotation marks on the "biology" term which will account for this assumption. The "biological" driven monthly pCO$_2$ change, ΔpCO$_{2,\text{bio}}$, has been calculated by

$$\Delta p\text{CO}_{2,\text{bio}} = \frac{7.2 \times \left(\text{NO}_{3,\text{m}} - \text{NO}_{3,\text{pm}}\right)}{\text{DIC}_{\text{mean}}} \times R \times p\text{CO}_{2,\text{pm}}, \quad (7)$$

where NO$_{3,\text{m}}$ and NO$_{3,\text{pm}}$ are the monthly mean surface layer nitrate concentrations of the month under consideration and the previous month, respectively. DIC$_{\text{mean}}$ is the annual mean value of dissolved inorganic carbon for each basin, R is the buffer factor calculated for each basin, and pCO$_{2,\text{pm}}$ denotes the observed monthly mean seawater pCO$_2$ of the previous month. Both, DIC$_{\text{mean}}$ and the buffer factor were calculated from the pCO$_2$, total alkalinity (TA), SST, and SSS annual mean data for each basin. The resulting buffer factor was slightly higher in the eastern (10.56) than in the western basin (10.02). The alkalinity data in turn are derived from the salinity observations (SSS$_{\text{obs}}$) based on a linear regression of discrete TA (μmol kg^{-1}) and SSS data collected over the sampling period,

$$\text{TA}\left(\mu\text{mol kg}^{-1}\right) = 50.78 \times \text{SSS}_{\text{obs}} + 527. \quad (8)$$

This regression compares very well with earlier observations [*Körtzinger et al.*, 2001; *Millero et al.*, 1998].

[23] In order to calculate the air-sea exchange effect on the observed monthly pCO$_2$ changes (ΔpCO$_{2,\text{ASE}}$), the observed pCO$_2$ data set was combined with climatological data for the mixed layer depth (MLD) and wind speed. Mixed layer depths are taken from the Levitus 1994 climatology [*Levitus and Boyer*, 1994] using the potential density criterion (change of 1.25×10^{-4} g cm^{-3} in potential density with respect to the surface value). We preferred this to the temperature criterion since it better corresponds to the water mass characteristics in the North Atlantic [see also *Kara et al.*, 2000]. Wind speed data are monthly mean averages from the COADS climatology. We used wind speeds and the transfer coefficient that is based on the long-term parameterization of *Wanninkhof* [1992] to calculate the monthly CO$_2$ flux F_{m}. Subsequently, the ΔpCO$_2$ associated with gas exchange is calculated,

$$F_{\text{m}} = k K_0 \left(p\text{CO}_{2,\text{air,m}} - p\text{CO}_{2,\text{sea,m}}\right) \quad (9)$$

$$\Delta p\text{CO}_{2,\text{ASE}} = R \times p\text{CO}_{2,\text{pm}} \times \frac{F_{\text{m}}/\text{MLD}}{DIC_{\text{mean}}}, \quad (10)$$

where R is the annual buffer factor for each basin, pCO$_{2,\text{m}}$ and pCO$_{2,\text{pm}}$ are the observed seawater pCO$_2$ of the current and the previous month, respectively, DIC is the annual
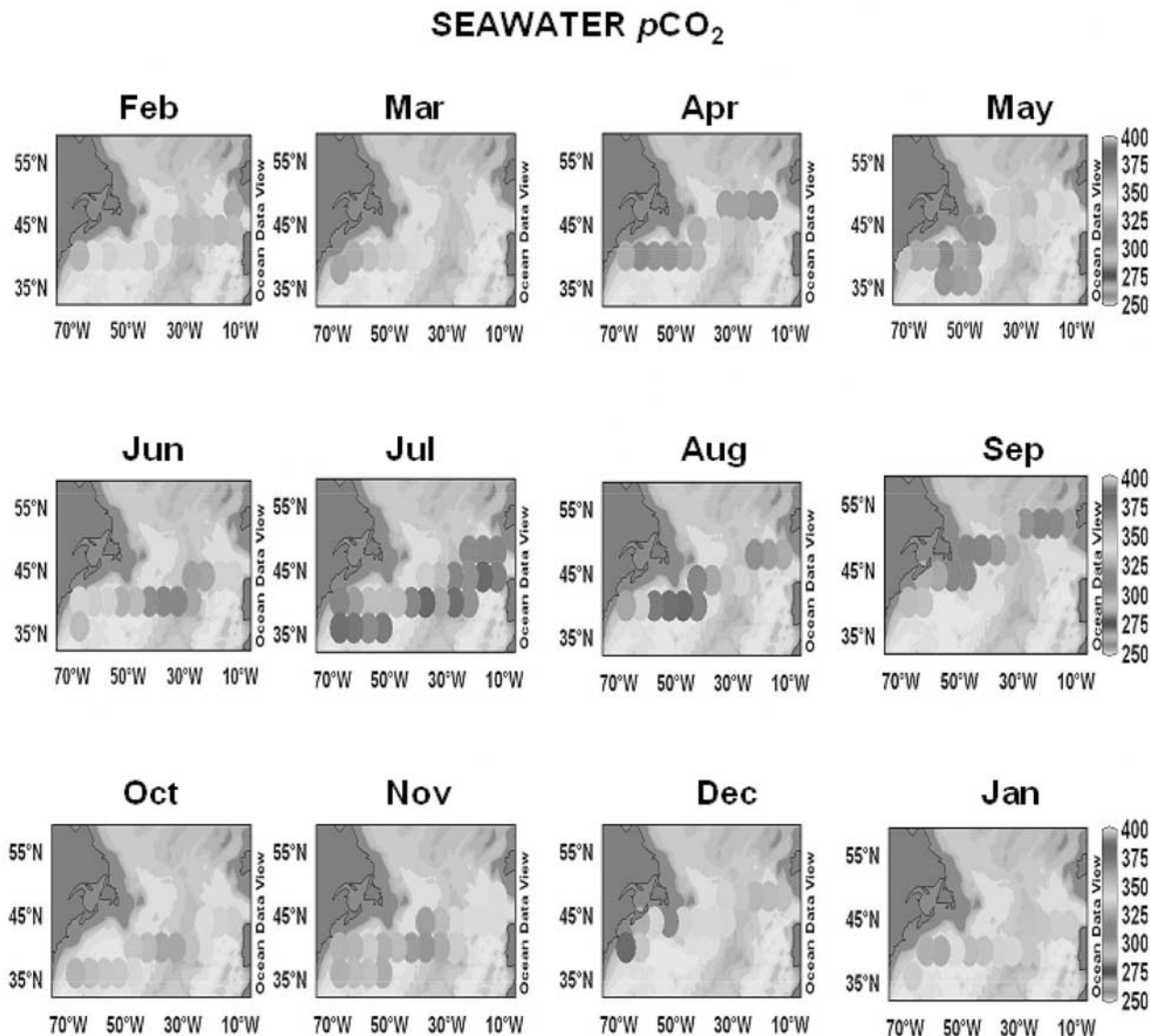
SEAWATER pCO_2

Figure 4. Monthly distribution of the seawater pCO_2 from February 2002 to January 2003. No data were recorded for the eastern basin in March 2002 due to technical problems. See color version of this figure at back of this issue.

mean value of the dissolved inorganic carbon for each basin, and MLD is the mixed layer depth.

3. Results

3.1. Seasonal Cycles of the Surface Seawater pCO_2, Temperature, and Nutrients

[24] Our data set permits calculation of monthly pCO_2 maps in the midlatitude North Atlantic for the period February 2002 to January 2003 (Figure 4). As explained above, we separated the observations into two provinces which are characterized by an opposite phase of the seasonal pCO_2 amplitude.

[25] Between January and March the seawater pCO_2 ranges between 320 and 340 μatm with slightly lower values in the western basin than in the eastern basin. In April the eastern basin still shows higher values around 350 μatm, while in the western basin values had dropped to 300–330 μatm, indicating an earlier onset of the productive season in the west. In May and June the seawater pCO_2 also started to decrease in the eastern basin (340–330 μatm), while western basin pCO_2 values increased slightly (325–335 μatm). From July to September the pCO_2 values rose significantly in the western basin as a consequence of seasonal warming. During the summer months the mean difference of pCO_2 between the eastern and western basins is about 30 μatm. In October and November the pCO_2 of both basins is distributed more uniformly with values around 340 μatm. In December the pCO_2 values are higher than in the previous 2 months, which is likely the result of
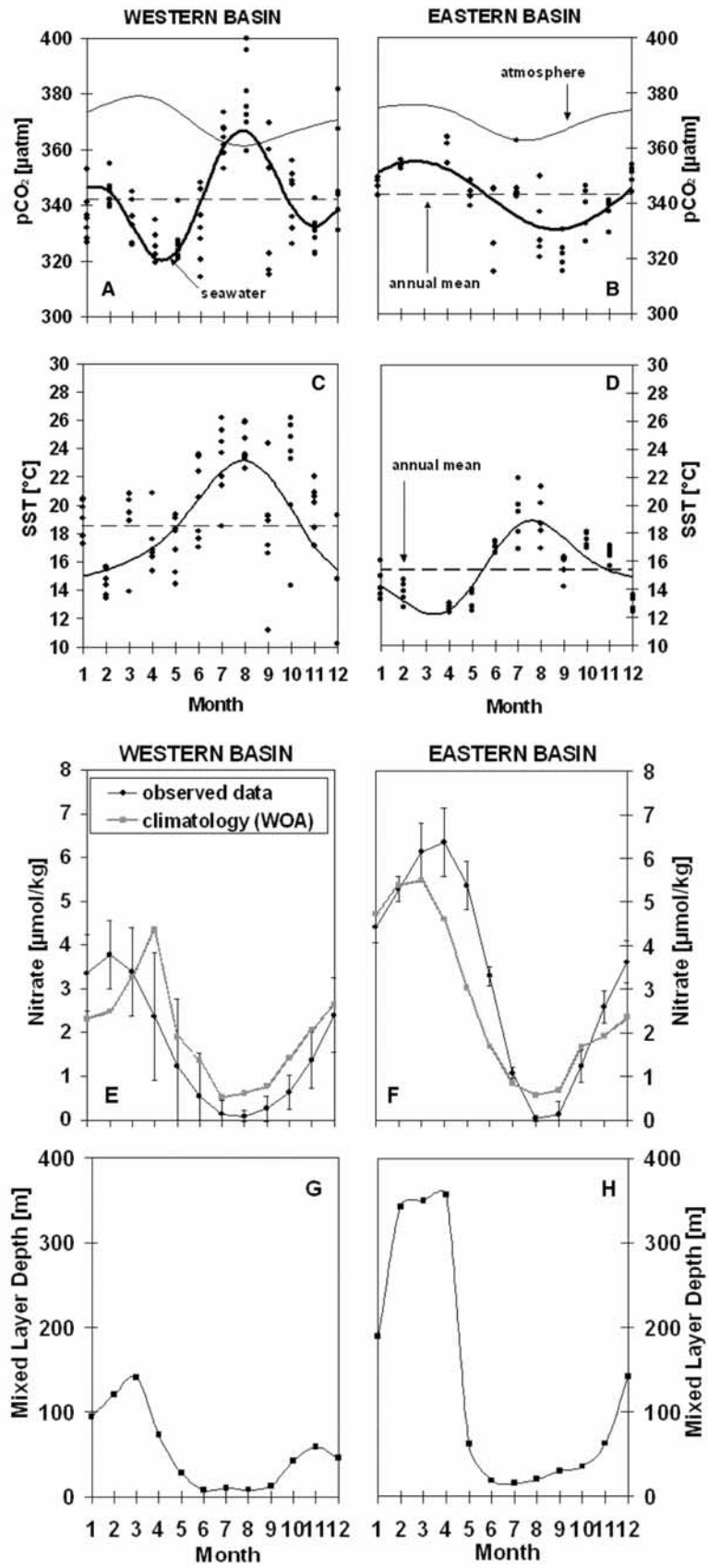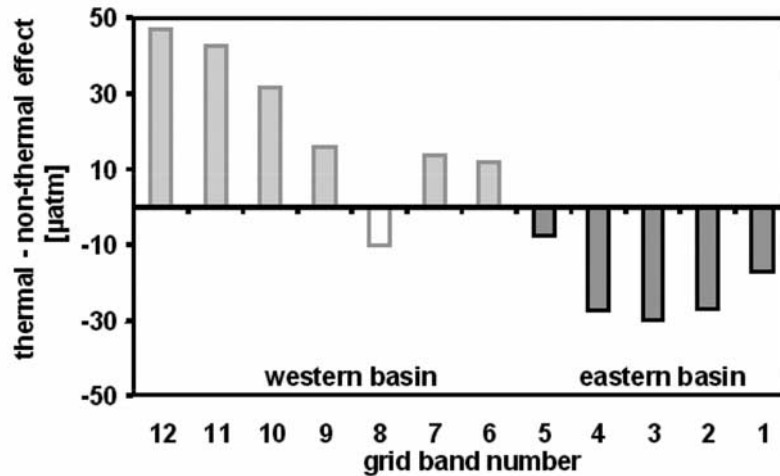
Figure 5

Figure 6. Difference between temperature and nontemperature related effects on the seawater pCO$_2$ for each grid band in the eastern and western basin as computed according to *Takahashi et al.* [2002].

vertical mixing entraining subsurface waters with elevated pCO$_2$.

[26] The western basin shows a higher variability of seawater pCO$_2$ than the eastern basin (Figures 5a and 5b); however, the annual pCO$_2$ means are nearly the same in the western (342 μatm) and in the eastern basin (343.2 μatm). Generally, the seawater pCO$_2$ is lower than the atmospheric pCO$_2$ (370.3 ± 5 μatm) except during the summer months, where surface waters in the western basin reach equilibrium and become supersaturated for a short period of time. Therefore the studied region (34°N–50°N) represents perennial sink for atmospheric CO$_2$ with the exception of the western basin during late summer. The SST data show similar patterns of variability (Figures 5c and 5d) for each basin, with higher seasonal amplitude in the western basin (14°C) than in the eastern basin (7°C) when calculated from the observed monthly means.

[27] The nitrate data (Figures 5e and 5f) show a higher seasonal nitrate drawdown (winter maximum − summer minimum) in the eastern basin (7 μmol kg^{-1}) than in the western basin (5 μmol kg^{-1}). The difference in the nutrient seasonality is also reflected in the World Ocean Atlas climatology [*Conkright et al.*, 2002], but it is not as pronounced. It is noticeable that the minimum nitrate concentrations of the climatology are higher than the observed concentrations. The seasonal signal (winter maximum − summer minimum) of the climatological nitrate data is reduced by 30–40% (western basin: 4 μmol kg^{-1}; eastern basin: 5 μmol kg^{-1}).

[28] The annual cycle of the mixed layer depth (MLD) shows a significantly higher seasonal amplitude in the eastern basin than in the western basin (Figures 5g and 5h).

In March and April the mixed layer deepens to maximum values of about 360 m and 140 m in the eastern and western basin, respectively. Beginning in May the MLD shallows and the minimum depths persist in the eastern and western basin until November and October, respectively.

3.2. Seasonal Controls on Surface Seawater pCO$_2$

[29] The difference $(T - B)$ between the thermal (T) and nonthermal (B) forcing was calculated in equations (4) and (5), respectively, according to *Takahashi et al.* [2002]. The eastern basin pCO$_2$ is dominated by nontemperature effects, whereas the western basin pCO$_2$ is strongly driven by temperature (Figure 6). Accordingly, the summer pCO$_2$ maximum in the western basin is due to the fact that temperature is the major force that drives the seawater pCO$_2$. In contrast, pCO$_2$ values are generally lower in the eastern basin during summer and highest during winter when strong vertical mixing brings up subsurface waters of pCO$_2$. This can be verified by the mixed layer climatology showing much higher mixed layer depths during wintertime in the eastern basin than in the western basin. We would like to stress again that the nonthermal component is not necessarily a monocausal but collects the effects of processes such as biological production/respiration, changes in alkalinity, and also physical processes like vertical mixing, advection, and air-sea exchange of CO$_2$.

[30] We estimated two of these nontemperature effects using the current data set: the "biological" carbon drawdown (ΔpCO$_{2,\text{bio}}$) and the air-sea exchange (ΔpCO$_{2,\text{ASE}}$). The "biological" carbon drawdown (new carbon production) is calculated from changes in the observed nitrate concentration. The air-sea exchange term is derived from

Figure 5. Seasonal cycles of the seawater and (a, b) atmospheric pCO$_2$, (c, d) SST, (e, f) nitrate, and (g, h) MLD in the eastern and the western basin. Shown are the monthly means (black dots) and the results of the computation fit in each basin. The MLD data are taken from a climatology [*Levitus and Boyer*, 1994]. The nitrate data are also compared to the World Ocean Atlas climatology [*Conkright et al.*, 2001].
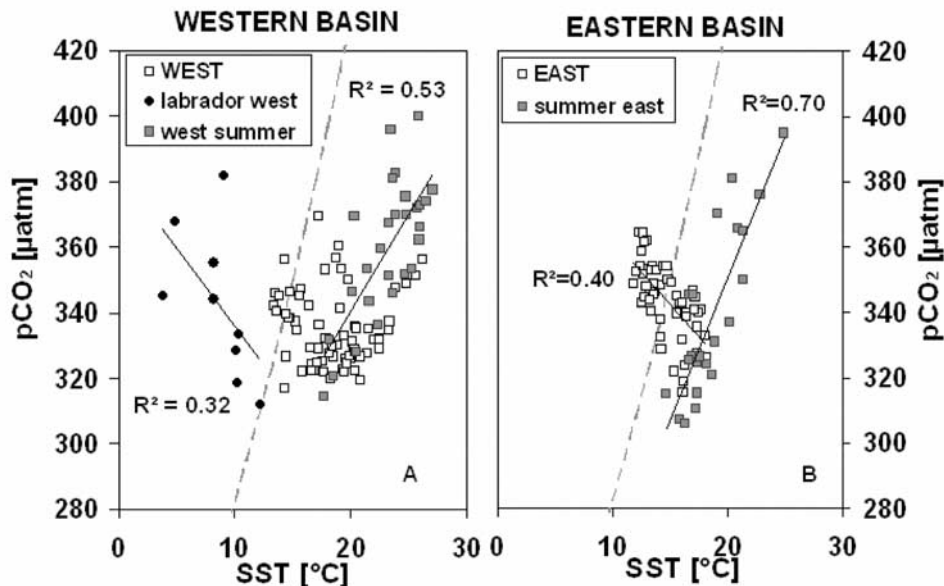
Figure 7. Property-to-property plot of SST and seawater pCO_2 for (a) the western and (b) the eastern basin. In the western basin we found no correlation between SST and pCO_2 (open squares, $R^2 = 0.00$) except for the following data subsets. We discriminate data with SST lower than 13°C, presumably belonging to Labrador Current (black dots) yielding: $y = -4.74x + 383.4$, $R^2 = 0.32$, and data observed in the summer months (shaded squares): $y = 5.94x + 221.59$, $R^2 = 0.53$. This relationship corresponds to 1.7% increase in pCO_2 per 1°C. In the eastern basin, data observed during the summer months (shaded squares) resulted in the following regression equation: $y = 8.71x + 176.83$, $R^2 = 0.70$ (2.51% °C^{-1}). The white squares represent the rest of the data set in the eastern basin which yielded: $y = -3.97x + 401.9$, $R^2 = 0.40$. Also shown is the isochemical line (dashed line) which describes the empirical relationship of 4.23% °C^{-1} between pCO_2 and SST that was determined for a North Atlantic seawater sample [*Takahashi et al.*, 1993].

the air-sea CO_2 flux which requires quantification of the air-sea ΔpCO_2 as well as MLD, wind speed, and the buffer factor of the marine CO_2 system. For calculation procedures, please refer to section 2.2.3.

[31] The seasonal amplitude of the seawater pCO_2 is less pronounced in the eastern basin compared to the western basin, and this can be inferred from the different forcing factors that influence the pCO_2 in each basin (Figure 9). In the eastern basin the subdued annual seawater pCO_2 cycle is a consequence of the seasonal $\Delta pCO_{2,temp}$ amplitude of 58 µatm, which is counterbalanced by the seasonal $\Delta pCO_{2,bio}$ amplitude of 44 µatm that is in almost exact opposite phase. The $\Delta pCO_{2,ASE}$ in the eastern basin always increases the pCO_2 except during March and April where the MLD is very deep and the effect is diluted. The strongest seasonal effect (20 µatm) is found during the summertime when the mixed layer depth is shallow and the CO_2 flux is therefore increased.

[32] In the western basin, the stronger seasonal ΔpCO_2 amplitude of 62 µatm is a consequence of a slightly stronger thermal forcing combined with a significantly smaller "biological" influence. The 50% lower "biological" carbon drawdown in the western basin is associated with a smaller nitrate amplitude, which in turn is driven largely by the MLD variability. The $\Delta pCO_{2,ASE}$ term is similar to the eastern basin except for the fact that net CO_2 flux becomes

negative (here: outgassing) in August when the seawater is oversaturated with respect to the atmosphere. It should be noted that the pronounced $\Delta pCO_{2,ASE}$ maximum in June is caused by an extremely shallow MLD of 8 m, which might be an artifact of the mixed layer depth climatology.

4. Discussion

4.1. pCO_2, SST, and Nutrient Variability in the Eastern and Western Basin of the North Atlantic

[33] Our data set compares well with earlier observations in this area. *Cooper et al.* [1998] reported 1 year of observations from a commercial vessel that was equipped with a pCO_2 measurement unit cruising from the UK to Jamaica between 1994 and 1995. They found the largest seasonal change of pCO_2 in the mid-Atlantic region (40°W–50°W) with summer supersaturation of pCO_2, which is consistent with our results. Furthermore, both data sets show that in the northeast Atlantic the seawater pCO_2 is undersaturated with respect to the atmosphere and therefore acts as a CO_2 sink.

[34] This data set covered the margins of both gyres, the subtropical and subpolar gyre. Hence the driving forces of the seawater pCO_2 will be influenced by these systems; however, the effects will be diluted. We found a positive correlation between temperature and pCO_2 in the western
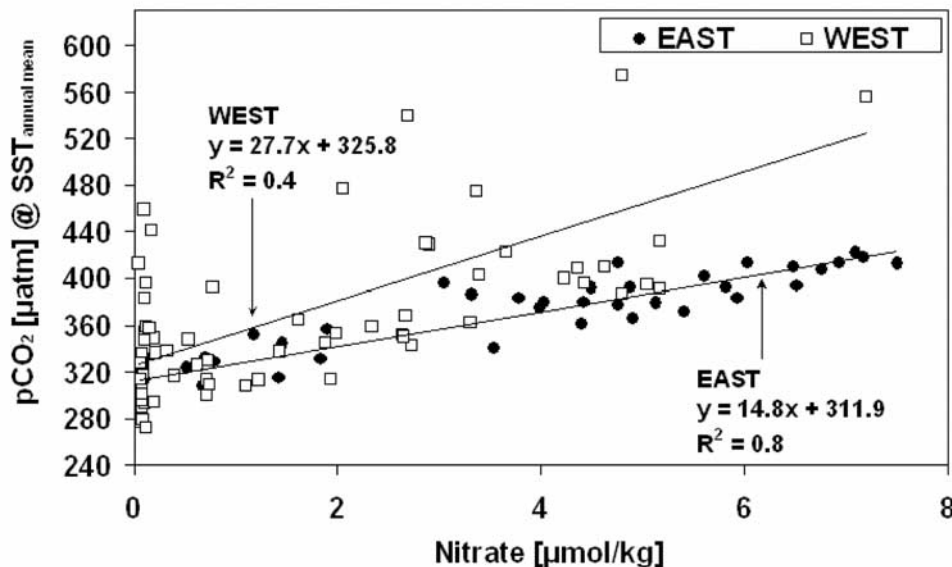
Figure 8. Property-to-property plot of nitrate versus seawater pCO_2 normalized to each basin's annual mean SST for the eastern (black dots) and the western basin (open squares). In the western basin, data from June until September with a nutrient concentrations of <0.12 μmol kg^{-1} are excluded as they yield no correlation with the pCO_2 data (summer depletion of nutrients).

and eastern basins for the summer months, which corresponds to a pCO_2 increase of ~1.7 and 2.5% per degree Celsius (Figure 7), respectively, which is comparable to *Cooper et al.* [1998], who observe a 2–3% °C^{-1} increase in pCO_2. The deviation from the thermodynamic effect (4.23% °C^{-1}) can mostly be explained by a counteracting "biological" effect (see below). SST was used earlier for the prediction of seawater pCO_2; however, our observations do not support this finding for seasons other than summer when stratification prevents the upward mixing of nutrients and limits biological production. A pCO_2 prediction by SST was successful in the center of the subtropical gyre [*Lefèvre and Taylor*, 2002; *Bates et al.*, 1998]. The observed water masses along our VOS line, however, include mixtures of surface water masses of different origins which are stronger influenced by biological activity, air-sea exchange, and vertical mixing/lateral advection than within the center of the subtropical gyre. If the summer months are excluded we find a weak negative correlation between SST and pCO_2 in both basins (Figure 7). It is noteworthy that minimum SSTs are much lower in the western basin, which can be attributed to Labrador current waters (SST < 13°C) based on the low-salinity signature. A negative correlation between SST and pCO_2 is typically an indicator of vertical mixing/upwelling, which brings to the surface colder waters with elevated pCO_2 levels (respiratory CO_2 from subsurface respiration).

[35] The nitrate data compare well with earlier publications; however, slight variations occur when our data set is compared to the World Ocean Atlas climatology. The latter shows a lower seasonal nitrate drawdown than our observed data, but *Takahashi et al.* [1993] report a seasonal nitrate drawdown of ~8 μmol kg^{-1} in the northeast Atlantic (47°N, 20°W) which is in the range of our observations in the eastern basin. Generally, the seasonal range of surface nutrients can be considerable owing to the interannual variability in mixing and especially biological productivity. In the eastern basin, which is mainly influenced by the North Atlantic drift, temperature-normalized seawater pCO_2 shows a strong correlation with nitrate ($r^2 = 0.8$; Figure 8). An explanation of the strong "biological" effect which is in essence derived from nitrate concentrations is the broad MLD range in the eastern basin. A maximum depth of over 300 m is reached which is caused by deep water convection and higher wintertime wind stress in this region. In the western basin the MLD is generally shallower, reflecting a higher stratification, especially during the summer months. In the subtropical gyre the nutrient concentrations are usually very low and the winter mixing produces a peak-like spring bloom through the upward transport of water masses that have higher nutrient concentrations [*Bates*, 2001]. Our observations in the western basin show a nutrient concentration throughout the year, except during the summer months, that is at least ten-fold higher than nitrate concentrations in the subtropical gyre (BATS site). Thus the analyzed region shows different nitrate patterns than the subtropical gyre, pointing toward a more mesotrophic system. When the summer months are excluded from the data, a weak correlation between temperature-normalized pCO_2 and nitrate is found in the western basin ($r^2 = 0.4$; Figure 8) which is only 50% of the correlation found for the eastern basin. In contrast to the pCO_2-SST correlation (excluding the summer months), the correlations with nitrate in both basins are positive. Since
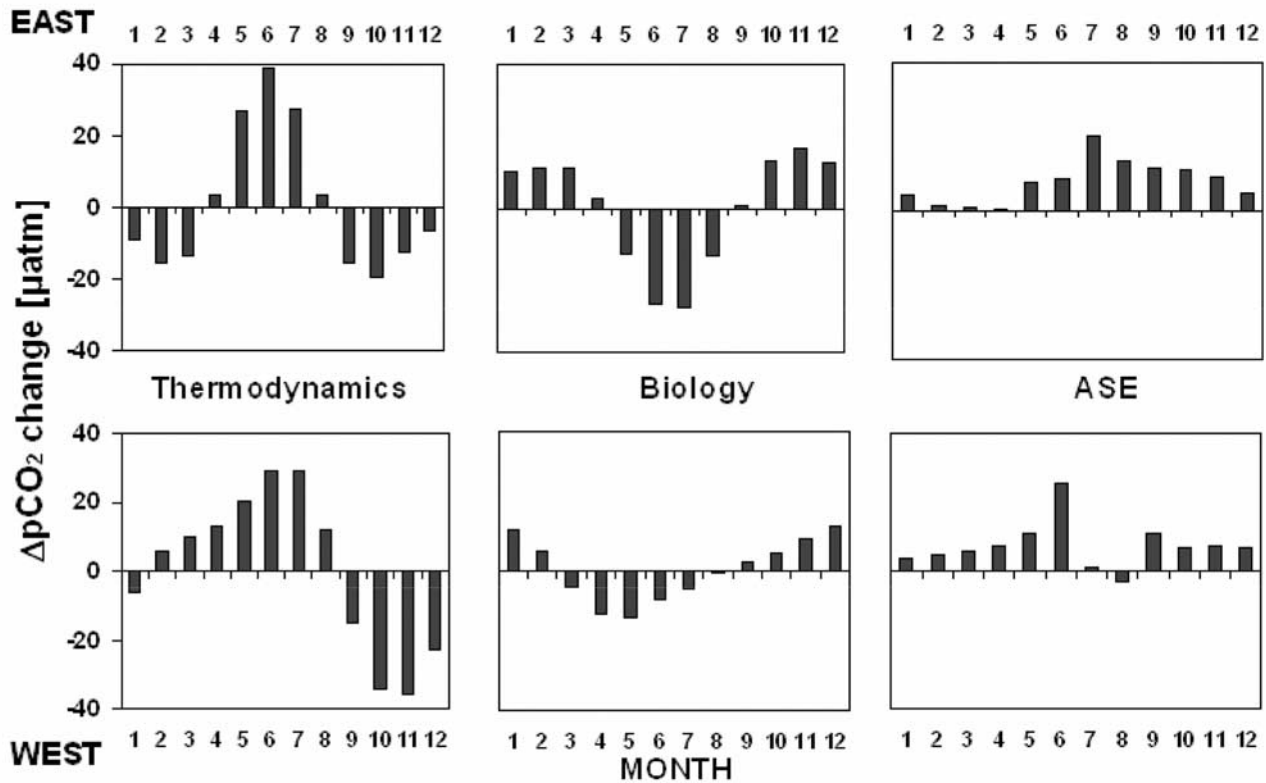
Figure 9. Monthly changes in surface ocean pCO_2 in the western and eastern basin as driven by (left) temperature changes ($\Delta pCO_{2,temp}$ = thermodynamics), (middle) biological carbon drawdown ($\Delta pCO_{2,bio}$ = Biology), and (right) air-sea CO_2 exchange ($\Delta pCO_{2,ASE}$ = ASE). For calculation procedures, please refer to the methods chapter.

nitrate and SST are also negatively correlated, the effects of temperature increase and ''biological'' drawdown (as mirrored in nitrate concentrations) on the seawater pCO_2 are counteractive, which is shown in Figure 9. *Lefèvre and Taylor* [2002] found that the strength of the biological effect increases with latitude in the subtropical gyre of the northeast Atlantic. Although our measurements were at the margins of the subtropical gyre, we can nevertheless confirm this finding in the regard that the $\Delta pCO_{2,bio}$ of the eastern basin is more pronounced than in the western basin. This is also based on the fact that the observations in the eastern basin are farther north than in the western basin. Concluding, we can show that in the western basin the temperature effect on the pCO_2 is not counteracted by an equally strong opposite ''biological'' effect, and as a consequence the seawater pCO_2 primarily follows temperature changes. This result is confirmed by model experiments which use data from various stations in the eastern and western North Atlantic. *Broström* [2000], for instance, shows that biology is more important for the pCO_2 in northern nutrient-rich parts than in the southern nutrient-depleted areas, whereas the SST influence is strongest in southern areas and relatively weak in northern areas.

[36] MLD not only affects the nitrate concentration through physical mixing, but it also plays an important role for the air-sea exchange (ASE). *Broström* [2000] explains

that the imprint of the ASE effect on the inorganic carbon concentration is strongest when the MLD is shallow and furthermore estimates the ASE effect to be 50% of the SST effect. This is in line with our findings, as we could show that the ASE effect is generally smaller than the thermodynamic and ''biological'' effect on the pCO_2. Hence the choice of the MLD data set is crucial and determining for the controls on the surface seawater pCO_2. It is difficult to assess the uncertainty of the MLD climatology, however, since it is highly variable in time and space. *Kara et al.* [2000] suggest that the variability of the MLD for any definition, for example, temperature or density criterions, yields an accuracy of only 20 m in 85% of the analyzed cases. In our case, for instance, a 10% decrease in MLD increases the $\Delta pCO_{2,ASE}$ term by 10%, which may lead to more significant contributions of this effect with respect to the pCO_2 variability.

[37] Earlier work suggested a good correlation between pCO_2 and chlorophyll [*Watson et al.*, 1991] since chlorophyll *a* has been used frequently as an indicator for algal biomass. The pCO_2 prediction from chlorophyll *a* would be very convenient as the latter can be remotely sensed. Our data, however, do not reveal any relationship between temperature-normalized pCO_2 and chlorophyll *a*, which is also true for remotely sensed chlorophyll data derived from the SeaWiFS project (Figure 10). There is no

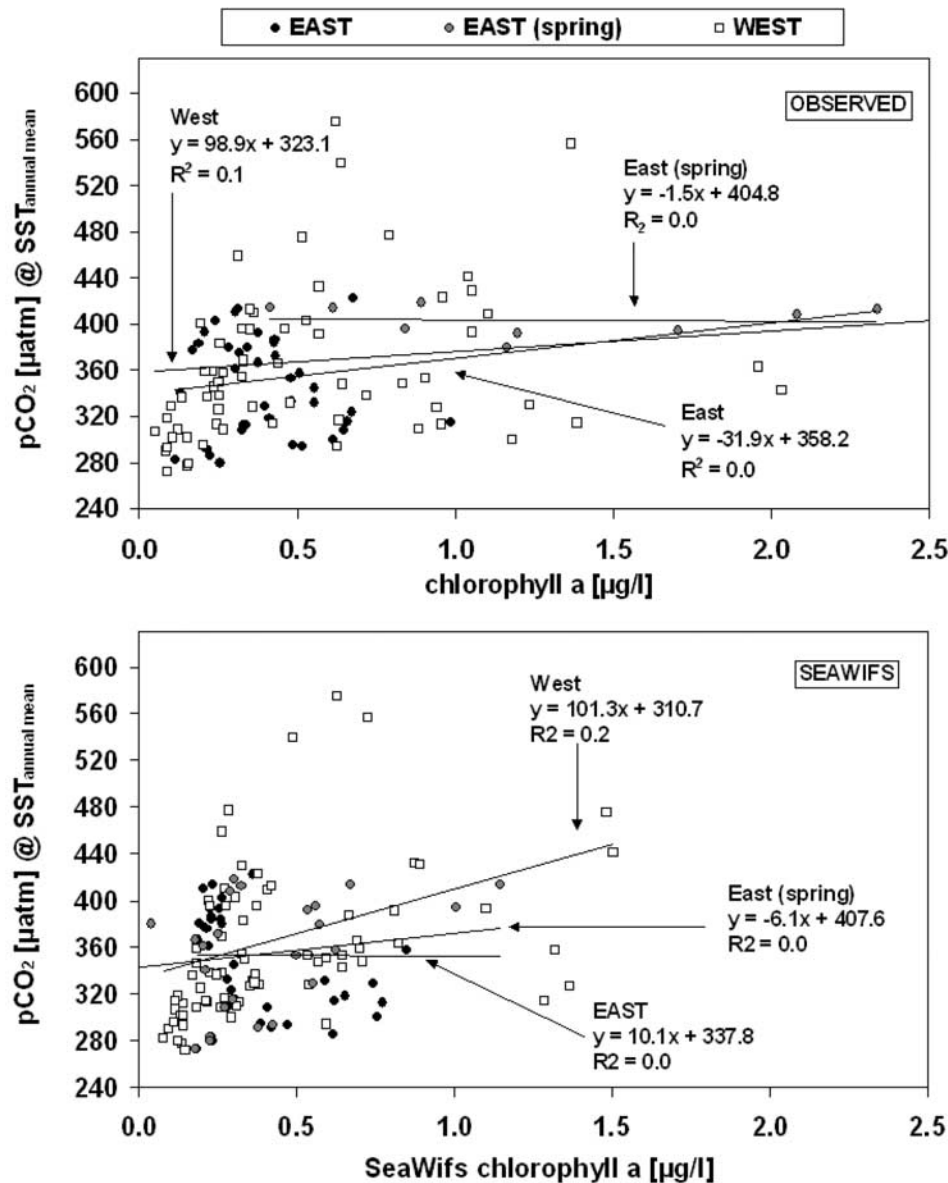**Figure 10.** Plot of (top) observed and (bottom) SeaWiFS chlorophyll *a* versus seawater pCO_2 normalized to each basin's annual mean SST for the eastern basin (black dots) and the western basin (open squares). In the eastern basin, spring data (April and May) are considered separately (shaded dots).

significant correlation in the present data set between pCO_2 and chlorophyll *a* for any region or time ($r^2 < 0.2$), not even for the spring bloom time where one might expect a closer relationship. Please note that the observed chlorophyll data generally compare well with the remotely sensed results except during spring and fall time where differences of more than 2 μg L^{-1} occur. It is most likely that the pCO_2-chlorophyll relationship is (1) very patchy, (2) probably obscured by variable and time-dependent chlorophyll-to-carbon ratios, and (3) to some extent masked by the large-scale effects of vertical mixing and variable water mass properties. On the basis of the present data set it is therefore not possible to confidently estimate the biomass and subsequently the seawater pCO_2 from chlorophyll *a*.

4.2. Comparison of pCO_2 Changes to the pCO_2 Climatology

[38] The measured annual cycles of seawater pCO_2 are compared to the climatological pCO_2 cycles of *Takahashi et al.* [2002]. Both data sets are corrected to the virtual year 1995 using the approach of *Takahashi et al.* [2002], who assumed that ocean areas south of 45°N should be corrected
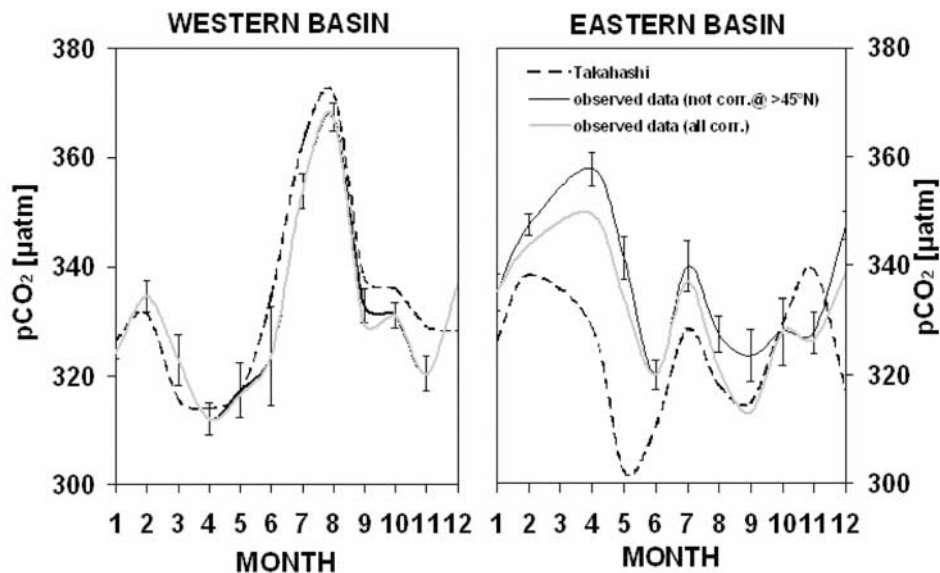
Figure 11. Comparison between measured (shaded line) and climatological pCO_2 data [*Takahashi et al.*, 2002] (dashed line). The observed data are corrected to 1995 assuming an annual increase of 1.5 ppm except for latitudes north of 45°N (dark shaded line). Also shown are the results where the correction to 1995 is applied to all data (light shaded line).

for the annual increase of anthropogenic CO_2 (C_{ant}) whereas areas north of 45°N would not show any long-term trends in surface ocean pCO_2. The latter assumption was derived from observations at Weather Station "P" (50°N, 145°W) in the northeastern subarctic Pacific by *Wong and Chan* [1991] where it was shown that the oceanic pCO_2 did not follow the atmospheric increase of CO_2. Here we corrected the observed pCO_2 data by using a correction factor of 1.5 ppm yr^{-1} for data south of 45°N, whereas data north of 45°N were left uncorrected for the anthropogenic increase (C_{ant}). Also shown is the result when all data (i.e., also those north of 45°N) are corrected for the anthropogenic CO_2 increase.

[39] In general, both data sets compare very well (Figure 11), especially in the western basin (annual mean observed-climatological pCO_2 difference = −2 μatm). Significant deviations between the observed year and the climatology are apparent mostly during the winter-spring season in the eastern basin. Here from January until May the observed pCO_2 is higher by ∼22 μatm than the climatological pCO_2 (annual mean observed-climatological pCO_2 difference = +13 μatm). In the eastern basin the agreement is slightly improved if we correct data north of 45°N for the temporal trends in atmospheric pCO_2. This discrepancy indicates that the sampled year may not be representative of the long-term climatological mean. It has been shown for the subtropical gyre near Bermuda that interannual variability of the upper ocean carbon cycle varies with the strength of the wintertime convection which was then extrapolated to the entire North Atlantic ocean [*Gruber et al.*, 2002]. We showed earlier that the pCO_2 variability strongly depends on the MLD, but the mechanisms that drive the annual pCO_2 cycle in the designated basins are of profound difference.

[40] The differences between the climatology and our data set are most likely caused by further implications. The first one relates to the fact that our data set only represents 1 year of data in contrast to *Takahashi et al.* [2002], who used over 900,000 data points for all oceans. Second, it is most likely that there is indeed an increase in C_{ant} in surface waters north of 45°N in contrast to the assumption by *Takahashi et al.* [2002]. Observations [*Omar et al.*, 2003] and models [e.g., *Anderson and Olsen*, 2002] show that the surface pCO_2 within this region did indeed increase; therefore it seems reasonable to apply the correction factor also to regions north of 45°N in the North Atlantic. Our findings also support a temporal trend in surface ocean pCO_2 north of 45°N, and therefore the assumption of *Takahashi et al.* [2002] does not appear to be valid for the North Atlantic.

5. Conclusions

[41] We successfully established a VOS-line in the North Atlantic on board the merchant vessel M/V *Falstaff* owned by the Swedish Wallenius Lines A/S. The measurements of seawater pCO_2 and further parameters started in February 2002 continued well into 2003.

[42] Our results suggest that in the eastern and the western basin the variability of the seawater pCO_2 is steered by different mechanisms. We show that along our transect, predicting the seawater pCO_2 from temperature might be successful in the summer, but the correlation of pCO_2 and SST is too weak during the rest of the year. Despite earlier observations, we showed that chlorophyll cannot be used as a predictor for pCO_2, as we could not prove any correlation between the two. However, our results are promising with regard to the relationship between nitrate and pCO_2. Here

the mixed layer depth which is strongly correlated with the nitrate supply might be an auspicious parameter to be used for pCO_2 predictions.

[43] The seasonal cycle of the seawater pCO_2 within the analyzed region and time is controlled by two major forcings: temperature and "biology." The latter includes physical mixing effects since the nutrient concentration is changed by both biology and vertical mixing, advection, eddies, etc. In the eastern basin the temperature and "biology" effect cancel each other and the overall effect is the observed subdued seasonal cycle of the seawater pCO_2. In the western basin the "biological" drawdown is gradual and it does not counteract the temperature effect; therefore it is more temperature controlled than the eastern basin. The effect of air-sea exchange is smaller compared to temperature and biology effects when the climatological MLD are used. Future analysis will test whether more accurately computed MLD data will change the ASE effect significantly.

[44] It is noteworthy to point out that the annual mean pCO_2 of both basins is the same despite the fundamental differences in underlying mechanisms. Related parameters such as SST, nutrients, and MLD may offer hindsight into these mechanisms as we showed in this work. It is difficult, however, to discriminate between true biological and physical controls that mediate the seawater pCO_2, since both effects are strongly correlated and prone to large interannual variability. Such a large data set with the rather high spatial and temporal coverage achieved by VOS-type operations has major advantages in resolving not only the seasonal but also the interannual variability of properties in large ocean regions. The continuation of scientific measurements onboard commercial vessels is highly recommended, as they provide valuable insight into the biogeochemical functioning of the ocean which cannot be achieved by research vessels only.

References

Anderson, L. A., and A. Olsen (2002), Air-sea flux of anthropogenic carbon dioxide in the North Atlantic, *Geophys. Res. Lett.*, *29*(17), 1835, doi:10.1029/2002GL014820.

Bates, N. R. (2001), Interannual variability of oceanic CO_2 and biogeochemical properties in the Western North Atlantic subtropical gyre, *Deep Sea Res., Part II*, *48*, 1507–1528.

Bates, N. R., A. M. Michaels, and A. H. Knap (1996), Seasonal and interannual variability of oceanic carbon dioxide species at the U.S. JGOFS Bermuda Time-series Study (BATS) site, *Deep Sea Res., Part II*, *43*, 347–383.

Bates, N. R., T. Takahashi, D. W. Chipman, and A. H. Knap (1998), Variability of pCO_2 on diel to seasonal timescales in the Sargasso Sea near Bermuda, *J. Geophys. Res.*, *103*(C8), 15,567–15,858.

Boutin, J., J. Etcheto, Y. Dandonneau, D. C. E. Bakker, R. A. Feely, H. Y. Inoue, M. Ishii, R. D. Ling, P. D. Nightingale, and N. Metzl (1999), Satellite sea surface temperature: A powerful tool for interpreting in situ pCO_2 measurements in the equatorial Pacific Ocean, *Tellus, Ser. B*, *51*, 490–508.

Broström, G. (2000), The role of the annual cycles for the air-sea exchange of CO_2, *Mar. Chem.*, *72*, 151–169.

Conkright, M. E., et al. (2002), *World Ocean Atlas 2001: Objective Analyses, Data Statistics, and Figures: Documentation* [CD-ROM], Natl. Oceanogr. Data Cent., Silver Spring, Md.

Cooper, D. J., A. J. Watson, and R. D. Ling (1998), Variation of pCO_2 along a North Atlantic shipping route (U.K. to the Caribbean): A year of automated observations, *Mar. Chem.*, *60*, 147–164.

Dandonneau, Y. (1995), Sea-surface partial pressure of carbon dioxide in the eastern equatorial Pacific (August 1991 to October 1992): A multivariate analysis of physical and biological factors, *Deep Sea Res., Part II*, *42*(2–3), 349–364.

Dickson, A. G., and C. Goyet (Eds.) (1994), DOE handbook of methods for the analysis of the various parameters of the carbon dioxide system in sea water, vers. 2, *Rep. ORNL/CDIAC-74*, Carbon Dioxide Inf. Anal. Cent., Oak Ridge Natl. Lab., Oak Ridge, Tenn.

Emery, W. J., and J. Meincke (1986), Global water masses: Summary and review, *Oceanol. Acta*, *9*(4), 383–391.

Etcheto, J., J. Boutin, Y. Dandonneau, D. C. E. Bakker, R. A. Feely, R. D. Ling, P. D. Nightingale, and R. Wanninkhof (1999), Air-sea CO_2 flux variability in the equatorial Pacific Ocean near 100°W, *Tellus, Ser. B*, *51*, 734–747.

Gruber, N., C. D. Keeling, and N. R. Bates (2002), Interannual variability in the North Atlantic Ocean carbon sink, *Science*, *298*, 2374–2378.

Hansen, H. P., and F. Koroleff (1999), Determination of nutrients, in *Methods of Seawater Analysis*, edited by K. Grasshoff, K. Kremling, and M. Ehrhardt, pp. 159–228, Verlag Chemie, Weinheim, Germany.

Hinrichsen, H.-H., and M. Tomczak (1993), Optimum Multiparameter analysis of the water mass structure in the western North Atlantic Ocean, *J. Geophys. Res.*, *98*(C6), 10,155–10,169.

Houghton, J. T., L. G. Meira Filho, B. A. Callender, N. Harris, A. K. Kattenberg, and K. Maskell (1996), *Climate Change 1995: The Science of Climate Change*, Cambridge Univ. Press, New York.

Jeffrey, S. W., and G. F. Humphrey (1975), New spectrophotometric equations for determining chlorophylls a, b, c_1, and c_2 in higher plants, algae and natural phytoplankton, *Biochem. Physiol. Pflanz.*, *167*, 191–198.

Johnson, K. M., A. Körtzinger, L. Mintrop, J. C. Duinker, and D. W. R. Wallace (1999), Coulometric total carbon dioxide analysis for marine studies: measurement and internal consistency of underway TCO_2 concentrations, *Mar. Chem.*, *67*, 123–144.

Kara, A. B., P. A. Rochford, and H. E. Hurlburt (2000), An optimal definition for ocean mixed layer depth, *J. Geophys. Res.*, *105*(C7), 16,803–16,821.

Körtzinger, A., W. Koeve, P. Kähler, and L. Mintrop (2001), C:N ratios in the mixed layer during productive season in the northeast Atlantic Ocean, *Deep Sea Res., Part I*, *48*, 661–688.

Lefèvre, N., and A. Taylor (2002), Estimating pCO_2 from sea surface temperatures in the Atlantic gyres, *Deep Sea Res., Part I*, *49*, 539–554.

Lefèvre, N., C. Andrié, and Y. Dandonneau (1994), pCO_2, chemical properties, and estimated new production in the equatorial Pacific in January–March 1991, *J. Geophys. Res.*, *99*(C6), 12,639–12,654.

Levitus, S., and T. Boyer (1994), *World Ocean Atlas*, vol. 4, *Temperature*, *NOAA Atlas NESDIS 4*, Natl. Oceanic and Atmos. Admin., Silver Spring, Md.

Millero, F. J., K. Lee, and M. Roche (1998), Distribution of alkalinity in the surface waters of the major oceans, *Mar. Chem.*, *60*, 111–130.

Mintrop, L., F. F. Pérez, M. G. Davila, J. M. S. Casiano, and A. Körtzinger (2000), Alkalinity determination by potentiometry—Intercalibration using three different methods, *Cienc. Mar.*, *26*, 23–37.

Nojiri, Y., Y. Fujinuma, J. Zeng, and C. S. Wong (1999), Monitoring of pCO_2 with complete seasonal coverage utilizing a cargo ship M/S Skaugran between Japan and Canada/US, in *Proceedings of the Second International Symposium of CO_2 in the Oceans*, CGER-Rep. CGER-I037-'99, pp. 17–23, Natl. Inst. for Environ. Stud., Tsukuba, Japan.

Omar, A., T. Johannessen, S. Kaltin, and A. Olsen (2003), Anthropogenic increase of oceanic pCO_2 in the Barents Sea surface water, *J. Geophys. Res.*, *108*(C12), 3388, doi:10.1029/2002JC001628.

Sasai, Y., M. Ikeda, and N. Tanaka (2000), Changes of total CO_2 and pCO_2 in the surface ocean during the mixed layer development in the northern North Pacific, *J. Geophys. Res.*, *105*(C2), 3465–3481.

Stephens, M. P., G. Samuels, D. B. Olson, and R. A. Fine (1995), Sea-air flux of CO_2 in the North Pacific using shipboard and satellite data, *J. Geophys. Res.*, *100*(C7), 13,571–13,583.

Takahashi, T., J. Olafsson, J. G. Goddard, D. W. Chipman, and S. C. Sutherland (1993), Seasonal variation of CO_2 and nutrients in the

high-latitude surface oceans: A comparative study, *Global Biogeochem. Cycles*, 7, 843–878.

Takahashi, T., et al. (2002), Global Sea-Air CO$_2$ flux based on climatological surface ocean pCO$_2$ and seasonal biological and temperature effects, *Deep Sea Res., Part II*, 49, 1601–1622.

Wallace, D. W. R. (2001), Storage and transport of excess CO$_2$ in the oceans: The JGOFS/WOCE Global CO$_2$ Survey, in *Ocean Circulation and Climate*, pp. 489–521, Academic, San Diego, Calif.

Wanninkhof, R. (1992), Relationship between wind speed and gas exchange over the ocean, *J. Geophys. Res.*, 97(C5), 7373–7382.

Watson, A., C. Robinson, J. Robinson, P. I. B. William, and M. Fasham (1991), Spatial variability in the sink for atmospheric carbon dioxide in the North Atlantic, *Nature*, 350, 50–53.

Weiss, R. F., R. A. Jahnke, and C. D. Keeling (1982), Seasonal effects of temperature and salinity on the partial pressure of CO$_2$ in seawater, *Nature*, 300, 511–513.

Winn, C. D., F. T. Mackenzie, C. J. Carillo, C. L. Sabine, and D. M. Karl (1994), Air-sea carbon dioxide exchange in the North Pacific Subtropical Gyre: Implications for the global carbon budget, *Global Biogeochem. Cycles*, 8, 157–163.

Wong, C. S., and Y.-H. Chan (1991), Temporal variations in the partial pressure and flux of CO$_2$ at Ocean Station P and Alert, Canada, *Tellus, Ser. B*, 43, 206–223.

Wright, W. R., and L. V. Worthington (1970), *The Water Masses of the North Atlantic Ocean: A Volumetric Census of Temperature and Salinity*, Ser. Atlas Mar. Environ., vol. 19, 8 pp., Am. Geogr. Soc., New York.

Yoder, J. A., and M. A. Kennelly (2003), Seasonal and ENSO variability in global ocean phytoplankton chlorophyll derived from 4 years of Sea-WiFS measurements, *Global Biogeochem. Cycles*, 17(4), 1112, doi:10.1029/2002GB001942.

Zeng, J., Y. Nojiri, P. P. Murphy, C. S. Wong, and Y. Fujinuma (2002), A comparison of ΔpCO$_2$ distributions in the northern North Pacific using results from a commercial vessel in 1995–1999, *Deep Sea Res., Part II*, 49, 5303–5315.

───────────────────

A. Körtzinger, H. Lüger, and D. W. R. Wallace, Marine Biogeochemie, Leibniz-Institut für Meereswissenschaften, Institute for Marine Research (IFM-GEOMAR), Düsternbrooker Weg 20, 24105 Kiel, Germany. (hlueger@ifm-geomar.de)

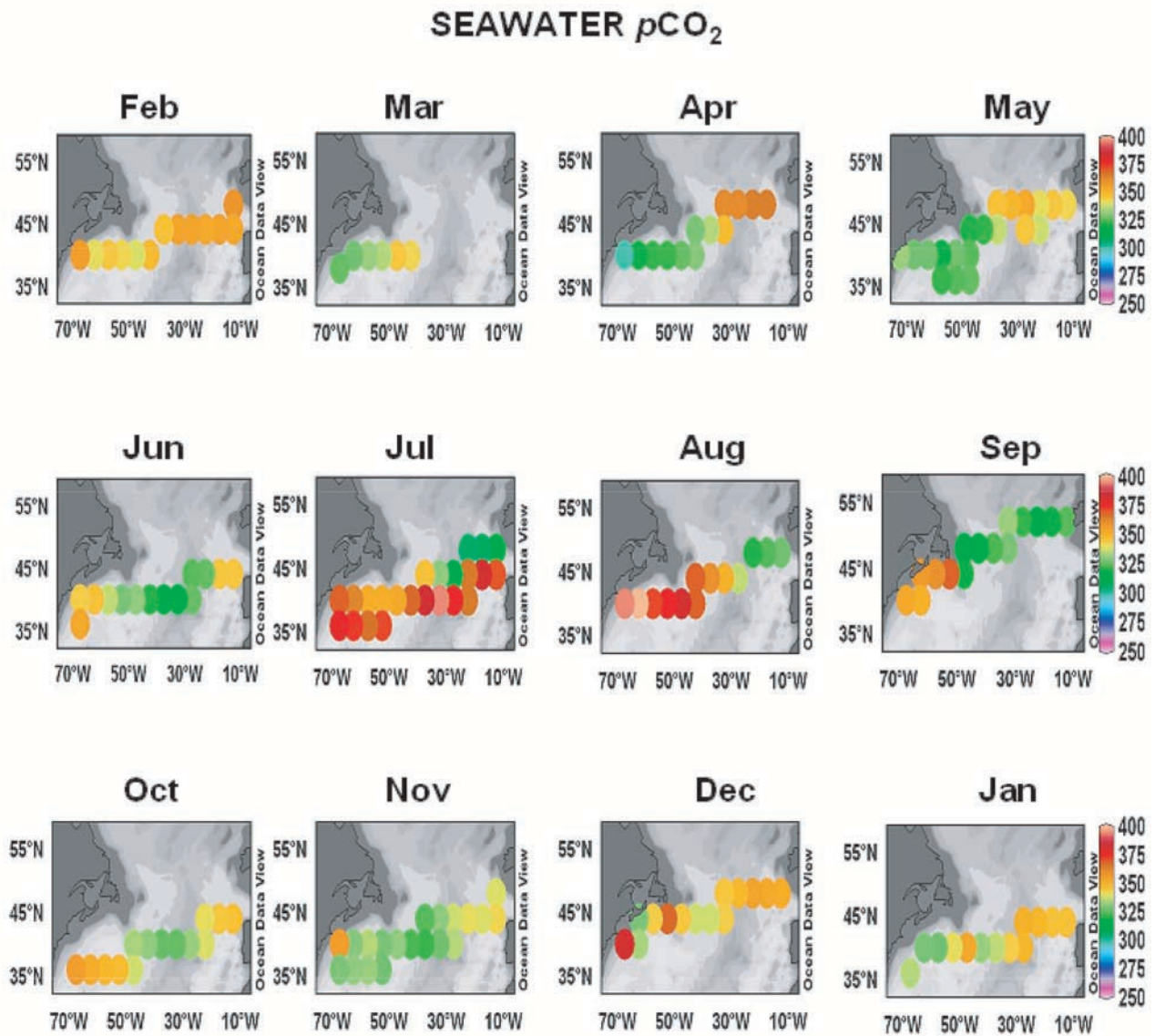Y. Nojiri, National Institute for Environmental Studies (NIES) 16-2, Onogawa, Tsukuba, Ibaraki, 305-0053, Japan.

Figure 4. Monthly distribution of the seawater pCO$_2$ from February 2002 to January 2003. No data were recorded for the eastern basin in March 2002 due to technical problems.